DISCRETE AND CONTINUOUS
DYNAMICAL SYSTEMS SERIES B
Volume **13**, Number **1**, January **2010**

doi:10.3934/dcdsb.2010.13.129

pp. **129–156**

STABILITY CROSSING BOUNDARIES OF DELAY SYSTEMS MODELING IMMUNE DYNAMICS IN LEUKEMIA

Silviu-Iulian Niculescu

Laboratoire des Signaux et Systèmes (UMR CNRS 8506)
Centre National de la Recherche Scientifique-Supélec
Gif-sur-Yvette, France

Peter S. Kim

Department of Mathematics
University of Utah
Salt Lake City, Utah, 84112-0900, USA

Keqin Gu

Department of Mechanical and Industrial Engineering
Southern Illinois University at Edwardsville
Edwardsville, Illinois, 62026-1805, USA

Peter P. Lee

Division of Hematology, School of Medicine
Stanford University
Stanford, California 94305, USA

Doron Levy

Department of Mathematics
and Center for Scientific Computation and Mathematical Modeling
University of Maryland
College Park, MD 20742, USA

(Communicated by Shigui Ruan)

2000 *Mathematics Subject Classification.* Primary: 34K20; Secondary: 92C50, 93D09, 93D99.

Key words and phrases. Delay, asymptotic stability, switch, reversal, crossing curves, quasipolynomial, leukemia models.

The research of S.-I. Niculescu was partially funded by a CNRS-USA Grant: "Delays in interconnected systems: Analysis, and applications" (2005–2008). The research of D. Levy was partially supported by the NSF under Career Grant DMS-0133511 and by the NSF/NIGMS program Grant DMS-0758374. The research of P.P. Lee was partially supported by a Research Scholar Award from the American Cancer Society. The research of D. Levy and of P.P. Lee was partially supported by Grant Number R01CA130817 from the National Cancer Institute. Part of the research of P.S. Kim was conducted during a Chateaubriand Postdoctoral Fellowship at the Laboratory of Signals and Systems.

Abstract. This paper focuses on the characterization of delay effects on the asymptotic stability of some continuous-time delay systems encountered in modeling the post-transplantation dynamics of the immune response to chronic myelogenous leukemia. Such models include multiple delays in some large range, from one minute to several days. The main objective of the paper is to study the stability of the crossing boundaries of the corresponding linearized models in the delay-parameter space by taking into account the interactions between small and large delays. Weak, and strong cell interactions are discussed, and analytic characterizations are proposed. An illustrative example together with related discussions completes the presentation.

1. **Introduction.** The stability analysis of population dynamics and of physiology models (especially, dynamic diseases) in the presence of time delays is a subject of recurring interest (see, for instance [25, 27, 29, 30] and the references therein). Time delays are often *inherent* in the model representation as certain processes such as maturity and gestation are never instantaneous. The presence of time delays may induce *complex behaviors* (instability, oscillations, and chaotic behaviors). The difficulty in analyzing time-delayed systems is mainly related to the fact that such systems are infinite-dimensional (see, e.g., [22]).

Various methods have been developed to analyze the dependence of stability on the time-delay parameters, and to compute the corresponding stability regions in terms of delays (see, e.g., [18, 31] and the references therein for an overview). Among them, we cite, for instance, the almost forgotten works of Lee and Hsu [26] on τ-decomposition method. Next, Stépàn [33] who provides a method to map the regions of delay space that correspond to stable solutions. Discussions of the Cooke and van den Driessche [13] method for characterizing the delay intervals guaranteeing stability can be found in [7, 25]. Some of its applications and extensions to biological models can be found in [4]. Campbell [9] also determines stability conditions and describes the bifurcations of a second-order delay differential equation for a damped harmonic oscillator. More recently, Olgac, Ergenc, and Sipahi developed a method called the cluster treatment of characteristic roots (CTCR) to identify multiple contiguous stable zones called stable "pockets" [32]. Their method is based on the so-called *pseudo-delay technique* (see also [27] for some discussions on such an approach). Finally, some classification of stability crossing boundaries and their characterization (analytical, computational) can be found in [19].

Several delay models have been recently developed to mathematically represent the dynamics of chronic myelogenous leukemia and of white blood cell development. In [5], Bernard, Bélair, and Mackey developed a DDE model for the production of neutrophils, and in [6], they presented a DDE model for the production of white blood cells. In [1], Adimy, Crauste, and Ruan developed a model of blood cell production using a system of age-structured partial differential equations that they convert to a system of nonlinear differential equations with distributed delay. In a model inspired by [5] and [6], Adimy, Crauste, and Ruan devised a model for white blood cell production using a system of delay differential equations (DDEs) [2]. In [12], Colijn and Mackey modeled periodic chronic myelogenous leukemia using a system of DDEs.

1.1. **Nonlinear delay model.** In this paper, we consider a simplification (and modification) of the nonlinear model proposed by [15, 23] to describe the post-transplantation dynamics of the immune response to chronic myelogenous leukemia

(CML). The original model from [15] tracks the time evolution of six cell populations (cancer cells, anti-donor T cells, general patient blood cells, anti-host T cells, anti-cancer T cells, and general donor blood cells). In our previous analysis, we found that the most important interaction is the interaction between the anti-cancer T cells from the donor and the cancer cells in the host [15]. Hence, to simplify the stability analysis, we consider the reduced system (1). This reduced system only considers the anti-cancer T cell population, $T(t)$, and the active and dying cancer populations, $C_A(t)$ and $C_D(t)$. The total population of cancer cells is denoted by $C(t)$, i.e., $C(t) = C_A(t) + C_D(t)$. All the other variables are constant and non-negative.

$$\begin{cases} \dfrac{dT(t)}{dt} = & -d_T T(t) - kC(t)T(t) + p_2 kC(t-\sigma)T(t-\sigma) \\ & +2^N p_1 q_1 kC(t-\rho-N\tau)T(t-\rho-N\tau) \\ & +p_1 q_2 kC(t-\rho-\upsilon)T(t-\rho-\upsilon), \\ \dfrac{dC_A(t)}{dt} = & rC_A(t)(1-C_A(t)/K) - \tilde{p}_1 kC_A(t)T(t), \\ \dfrac{dC_D(t)}{dt} = & \tilde{p}_1 kC_A(t)T(t) - \tilde{p}_1 kC_A(t-\rho)T(t-\rho). \end{cases} \tag{1}$$

A time-delay model offers a unique advantage in immune system modeling, because delays provide means for dealing with programmed T cell responses. When stimulated by a target, T cells undergo a program of division even if the original stimulation is removed [11]. Thus, the overall immune response at a given time is not dependent upon the current level of the stimulus, but on the level at some time in the past [28].

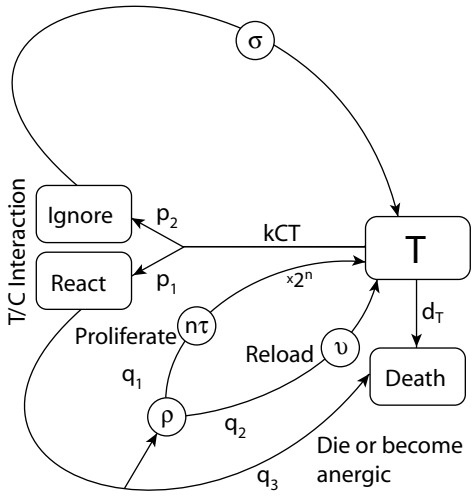

FIGURE 1. Evolution of anti-cancer T cells

The stages of the evolution of anti-cancer T cells are demonstrated in Figure 1. These cells interact with the cancer population, C. Based on the law of mass action, we assume that cancer/T cell interactions occur at a rate of kTC, where k is a

kinetic constant and T and C are the concentrations of the T cell and cancer population, respectively. In the T/C interaction, the T cells examine cancer cells and decide whether to react to the stimulus or to ignore it with probabilities $p_1^{T/C}$ and $p_2^{T/C}$, respectively. If the T cells ignore the stimulus, they return to the base state after a delay of σ, which represents the time for a non-productive interaction. If the T cells react, they have a chance of destroying the targeted cancer cell through a cytotoxic response associated with a delay of ρ. After responding, the cells may enter a cycle of proliferation with probability $q_2^{T/C}$. Alternatively, they may forego the proliferation plan and simply recover cytotoxic capabilities (involving the replenishing of cytotoxic granulocytes) in preparation for their next encounter, returning them to the pool of active cells after a delay of υ.

We assume that T cells divide an average of n times during proliferation, resulting in 2^n times as many cells. Each cycle of division takes τ units of time to complete, hence the entire proliferation cycle requires $n\tau$ units of time. We assume that during this time, all proliferating T cells are unavailable to interact with other cells, and thus they are not included in the measure of T. When interacting with cancer cells, there is a probability $q_3^{T/C}$ that the T cells will become anergic (i.e. tolerant) from the interaction. This effectively amounts to death in our simulations.

The equations presented in (1) for the cancer populations, C_A and C_D, are a modification of the original DDE system in [15]. In the DDE system of [15], the cancer population C might become negative since the second term of the equation for dC/dt (in [15]) does not directly involve the value of $C(t)$. As done in [15], this issue can be handled by imposing a stopping criterion that forces the derivative dC/dt to vanish, when C equals 0. This approach complicates the stability analysis.

As an alternative adjustment, in this paper, we divide the cancer populations into two subpopulations: active cancer cells, C_A, and dying cancer cells, C_D. When an interaction between an active cancer cell and a T cell results in a cytotoxic response, the cancer cell moves to the dying state. This event occurs with probability $\tilde{p}_1$. Dying cancer cells are not eliminated immediately, but remain for an additional ρ time units, before being removed. During this time, dying cells no longer proliferate, but may continue to stimulate circulating T cells [10]. The stages of the evolution of cancer cells are demonstrated in Figure 2.

In the equation for the T cell population, we define the total cancer population C to be the sum, $C_A + C_D$, of the two cancer sub-populations. In addition, active cancer cells, C_A, multiply at a logistic growth rate indicated by the closed loop at the top of Figure 2. The logistic parameter r represents the net growth rate of cancer. As shown in (1), we denote the carrying capacity of the cancer population by the variable K.

Furthermore, we assume the past history is constant before time 0. In other words, we set

$$T(t) = T_0, \qquad C_A(t) = C_{A,0}, \qquad C_D(t) = C_{D,0}, \qquad \text{for } t \le 0,$$

where the following compatibility condition holds:

$$C_{D,0} = \rho \tilde{p}_1 k C_{A,0} T_0. \tag{2}$$

The compatibility condition follows by noticing that when T and C_A remain constant, the equation for $C_D(t)$ in (1) implies (2).

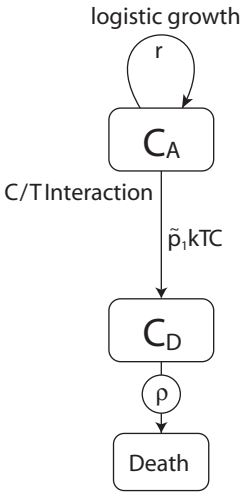

FIGURE 2. Evolution of cancer cells, C, in the modified model.

Note that condition (2), although biologically reasonable, is technically stronger than necessary. In fact, the more general condition

$$C_D(0) = \tilde{p}_1 k \int_{-\rho}^{0} C_A(u)T(u)du \tag{3}$$

applies to any biologically reasonable (e.g., continuous and nonnegative) choice of past history for C_A and T. This condition also guarantees the nonnegativity of $C_D(t)$. Indeed, from (1), we obtain

$$C_D(t) = \left[C_D(0) - \tilde{p}_1 k \int_{-\rho}^{0} C_A(u)T(u)\right] + \tilde{p}_1 k \int_{t-\rho}^{t} C_A(u)T(u)du,$$

and (3) implies that the constant term above equals 0. The nonnegativity of $T(t)$ and $C_A(t)$ is guaranteed by the form of (1).

Hence, unlike [15], in the modified model of this paper, cancer populations no longer require a stopping criterion to remain nonnegative. Hence, we can perform a more reasonable stability analysis.

1.2. **Delay description.** In the system (1) there are *four distinct delays*, namely σ, $\rho + N\tau$, $\rho + \upsilon$, and ρ. These constants respectively represent the time for non-reactive interactions between T cells and cancer cells (σ), the time for reactive interactions (ρ), the time for one round of cell division (τ), the T cell recovery time after killing a cancer cell (υ), and the average number of T cell divisions after stimulation (N).

The relevant values, taken from [15], are approximately

1. $\sigma = 0.0007$ days $= 1$ min
2. $\rho = 0.0035$ days $= 5$ min
3. $\tau = 1$ day
4. $\upsilon = 1$ day
5. N is between 1 and 8 and probably close to 3.

The model includes multiple delays in a large range starting from one minute up to several days. Due to the scale difference, we can define without any loss of generality ρ and σ as *small delays*, and the remaining delays as *large*.

1.3. **Stability analysis.** Stability analysis is appropriate for this model, because a stable solution may imply full remission of cancer or at least a state in which the cancer cells remain controlled. On the other hand, an unstable solution implies the eventual relapse of the cancer population, corresponding to an unsuccessful transplant.

The model we are analyzing contains four delays, two large delays and two small delays. Various methods have been developed to study multiple delay systems. For example, in [2], Adimy *et al.* analyze a two-delay system by first setting the smaller delay to 0 and then analyzing the stability of the larger delay. After determining the stable range for the larger delay while the smaller delay is set to 0, they determine the permissible range of the smaller delay that preserves the stability of the system. This sequential approach is useful for two-delays, but it is usually too difficult for more delays, in our case four. Furthermore, in our case, the approach is limited, because one cannot get a global perspective of the stability regions in the delay parameter space. In particular, one will only be able to map out a mostly convex subset of the stable region around the origin and will not be able to map out isolated pockets of stability in delay space. As another approach, in [6], Bernard *et al.* apply the Matlab package DDE-BIFTOOL [17] to analyze the dependence of white blood cell dynamics and hematopoietic stem cell dynamics on several non-delay parameters.

One of the main goals of our paper is to present a method for simultaneously analyzing four delays. Furthermore, this method suggests a natural generalization to higher numbers of delays. The approach treats all delays in a similar manner, whether large or small, and geometrically obtains a global map of stability regions throughout the entire delay parameter space.

For our particular application, we are interested in analyzing the *effects* induced by the *presence of delays* on the (asymptotic) stability of the corresponding linearized model, and more explicitly to derive the *stability/instability mechanisms* in the delay-parameter space. At the same time, we are interested in understanding the way small delays interact with large delays in defining stability/instability properties.

The method we are proposing is *intuitive*, easy to understand and *extremely* easy to *apply*. It is based on some simple properties of triangle geometry combined with continuity properties of the spectrum with respect to the delay parameters. It is important to note that such a method can be adapted to systems with a more complicated dynamics.

1.4. **Crossing boundaries.** One of the natural ideas to perform stability analysis is the computation of the stability (crossing) boundaries corresponding to the existence of some roots of the characteristic equation associated with the linearized system on the imaginary axis.

It is well known from the literature that such a stability characterization problem is still *open* in the general linear case (see, for instance, [16]), and that it is $\mathcal{NP}$-hard from the computational point of view [34]. However, the *particular structure* of the system, together with the particular way in which the *delays* appear in the differential equations of the model, allow the *characterization* of the stability

crossing boundaries in the delay-parameter space, that is their classification and explicit computation.

1.5. **Delay interactions and related measures.** As presented above (nonlinear model), the large delays $N\tau$, and υ describe the *T/C interactions*. Without any loss of generality, we can define two types of interactions: *weak*, and *strong* T/C interactions. The *weak interaction* simply corresponds to the situation when the large delays $N\tau$, and υ have a very low impact on the stability behavior, and the stability property will be very sensitive to the parameter variations of the small delay values. On the other hand, the *strong interaction* will describe the situation in which the stability of the model is *sensitive* also to the large delays $N\tau$, and υ. Connections with delay-independent/delay-dependent (stability) type properties will be also presented.

Based on these simple remarks, it seems that *strong T/C interactions* will be more difficult to characterize, and are more interesting. Finally, it is important to point out that an increased (average) number of T cell division after stimulation will significantly affect the behavior of the crossing boundaries, and the T/C interactions become more significant. In order to complete the presentation, a *measure* for *weak T/C interactions* will be derived. Such a measure will be *computationally tractable*, and will allow *defining* properly the cases when a T/C interaction has a *weak* or *strong character*. In other words, we will have a lower (upper) bound for defining strong (weak) T/C interactions.

1.6. **A geometric approach.** As seen below, we can rewrite the linearized model in some nice and appealing way that allows using a simple *geometrical idea* (as suggested by some of the authors of this paper in [19] for some class of quasipolynomials including two *independent* delays) for defining the frequency crossing set (all frequencies corresponding to all the points in the stability crossing curves). It is important to note that the approach in [19] cannot be applied directly to the case under consideration, and the definition of the *crossing set* here is more complicated. However, as we shall see later, the stability crossing set consists, under appropriate assumptions, of a *finite number* of *intervals* of *finite length* even in such a case, a fact that significantly simplifies the analysis.

Next, this crossing set will allow the characterization of the *stability crossing curves* in the delay-parameter space defined by the large delays υ, and $N\tau$, that is a series of smooth curves except for some degenerate cases to be considered.

The classification of the boundaries has some similarity to [19] (see Section 3). The novelty with respect to [19] is the use of more general analytic functions, and the particular way to treat the *small delays* σ, and ρ. Furthermore, the approach considered here will allow the analytic characterization of weak/strong T/C interactions. As mentioned above, we will give the explicit computation of some quantitative measure that characterizes weak T/C interaction.

1.7. **Paper outline.** The presentation will be as simple as possible, focusing on the main mathematical ideas. We will emphasize the related interpretations of the results in terms of the specific application to the post-transplantation dynamics of the immune response to chronic myelogenous leukemia. However, our mathematical ideas suggest possible extensions to a more general context and may be applicable to other systems as well.

The remaining part of the paper is organized as follows: Section 2 is devoted to deriving the linearized system and to obtaining some preliminary results on it. The

main results are presented in Section 3. We distinguish between weak and strong T cell – cancer cell interactions based on the probability of such interactions, and study the stability of the linearized system in both regimes. What is particularly challenging is the number of time-delays and our results are aimed in understanding the role that the small delays play on the stability of the system. An illustrative example is detailed and discussed in Section 4. Finally, some concluding remarks end the paper in Section 5.

2. **The linearized system: Preliminary results.** We start by deriving the linearized model of the system (1) and study its stability in the delay-free case. The particular structure of the linearized model leads to a nice form of the corresponding characteristic equation in the presence of delays. Its structure will allow us to define an appropriate *auxiliary system* with only the *small delays* needed in the next section to complete the analysis. For convenience, let

$$\begin{array}{lll} b_1 = d_T, & b_5 = p_1 q_2 k, & \tilde{\tau} = \rho + N\tau, \\ b_2 = k, & c_1 = r, & \tilde{\upsilon} = \rho + \upsilon, \\ b_3 = p_2 k, & c_2 = r/K, & \\ b_4 = 2^N p_1 q_1 k, & c_3 = \tilde{p}_1 k, & \end{array} \tag{4}$$

and rewrite (1) as

$$\left\{ \begin{array}{rcl} \dfrac{dT(t)}{dt} & = & -b_1 T(t) - b_2(C_A(t) + C_D(t))T(t) \\ & & +b_3(C_A(t-\sigma) + C_D(t-\sigma))T(t-\sigma) \\ & & +b_4(C_A(t-\tilde{\tau}) + C_D(t-\tilde{\tau}))T(t-\tilde{\tau}) \\ & & +b_5(C_A(t-\tilde{\upsilon}) + C_D(t-\tilde{\upsilon}))T(t-\tilde{\upsilon}), \\ \dfrac{dC_A(t)}{dt} & = & c_1 C_A(t) - c_2 C_A(t)^2 - c_3 C_A(t)T(t), \\ \dfrac{dC_D}{dt} & = & c_3 C_A(t)T(t) - c_3 C_A(t-\rho)T(t-\rho). \end{array} \right. \tag{5}$$

We note that all parameters in (4) are positive. Let $b = -b_2 + b_3 + b_4 + b_5$. Then the fixed points, $(T_0, C_{A,0}, C_{D,0})$, of (5) are solutions to

$$\left\{ \begin{array}{ll} 0 & = -b_1 T_0 + b(C_{A,0} + C_{D,0})T_0 = (-b_1 + b(C_{A,0} + C_{D,0}))T_0, \\ 0 & = (c_1 - c_2 C_{A,0} - c_3 T_0)C_{A,0}. \end{array} \right.$$

Note from (5) that since $C_{A,0}$ and T_0 are constant, we have $C_{D,0} = \rho c_3 C_{A,0} T_0$ (see (2)), so

$$\left\{ \begin{array}{ll} 0 & = (-b_1 + b(1 + \rho c_3 T_0)C_{A,0})T_0, \\ 0 & = (c_1 - c_2 C_{A,0} - c_3 T_0)C_{A,0}. \end{array} \right.$$

From these equations, we immediately calculate two fixed points $(T_0, C_{A,0}, C_{D,0})$ given by $(0,0,0)$, $(0,K,0)$. In the case where $T_0 \neq 0$, we obtain the quadratic equation

$$\rho b c_3^2 T_0^2 + b c_3(1 - \rho c_1)T_0 + b_1 c_2 - b c_1 = 0. \tag{6}$$

This means that we can determine $C_{A,0}$ and $C_{D,0}$ by the following equations:

$$\left\{ \begin{array}{l} C_{A,0} = (c_1 - c_3 T_0)/c_2, \\ C_{D,0} = \rho c_3 C_{A,0} T_0. \end{array} \right. \tag{7}$$

Hence, the system may contain up to two additional fixed points, for a total of between 2 and 4 fixed points, depending on the coefficients of (6).

The fixed point $(0,0,0)$ represents the ideal outcome, where the cancer population is entirely eliminated and the cancer-reactive T cells become unnecessary and disappear. Unfortunately, we will later show that this fixed point is a *saddle* regardless of the values of the parameters, which means that this fixed point is unattainable.

The fixed point $(0,K,0)$ represents the case where cancer expands to its carrying capacity, K, and the cancer-reactive T cells die off completely. This is the most undesirable state, and we will later show that the fixed point is *unstable* for biologically reasonable parameter choices.

The fixed points determined by (6) represent the scenarios where the cancer and T cell populations coexist. This means that cancer is not entirely eliminated, but is controlled in part by the immune response. For biologically reasonable parameters, we will show that this state can be *stable* for appropriate values of the delays. Such a case study will be considered in Section 4.

To study the stability of (5), we linearize the nonlinear system around the fixed point $(T_0, C_{A,0}, C_{D,0})$ and obtain

$$\begin{cases} \dfrac{dT(t)}{dt} = & -\tilde{b}_1 T(t) - b_2 T_0 (C_A(t) + C_D(t)) \\ & +b_3 (C_{A,0} + C_{D,0}) T(t-\sigma) + b_3 T_0 (C_A(t-\sigma) + C_D(t-\sigma)) \\ & +b_4 (C_{A,0} + C_{D,0}) T(t-\tilde{\tau}) + b_4 T_0 (C_A(t-\tilde{\tau}) + C_D(t-\tilde{\tau})) \\ & +b_5 (C_{A,0} + C_{D,0}) T(t-\tilde{\upsilon}) + b_5 T_0 (C_A(t-\tilde{\upsilon}) + C_D(t-\tilde{\upsilon})), \\ \dfrac{dC_A(t)}{dt} = & \tilde{c}_1 C_A(t) - c_3 C_{A,0} T(t) - c_3 T_0 C_A(t), \\ \dfrac{dC_D(t)}{dt} = & c_3 C_{A,0} T(t) + c_3 T_0 C_A(t) - c_3 C_{A,0} T(t-\rho) - c_3 T_0 C_A(t-\rho), \end{cases} \tag{8}$$

where $\tilde{b}_1 = b_1 + b_2(C_{A,0} + C_{D,0})$ and $\tilde{c}_1 = c_1 - 2c_2 C_{A,0}$.

2.1. **Linearized model in the presence of delays.** The characteristic equation of (8) is $\det(A(e^{-s}) - sI) = 0$, where

$$\begin{aligned} A_{11}(e^{-s}) &= -\tilde{b}_1 + b_3(C_{A,0} + C_{D,0})e^{-\sigma s} + b_4(C_{A,0} + C_{D,0})e^{-\tilde{\tau} s} \\ &\quad + b_5(C_{A,0} + C_{D,0})e^{-\tilde{\upsilon} s}, \\ A_{12}(e^{-s}) &= -b_2 T_0 + b_3 T_0 e^{-\sigma s} + b_4 T_0 e^{-\tilde{\tau} s} + b_5 T_0 e^{-\tilde{\upsilon} s}, \\ A_{13}(e^{-s}) &= -b_2 T_0 + b_3 T_0 e^{-\sigma s} + b_4 T_0 e^{-\tilde{\tau} s} + b_5 T_0 e^{-\tilde{\upsilon} s}, \\ A_{21}(e^{-s}) &= -c_3 C_{A,0}, \\ A_{22}(e^{-s}) &= \tilde{c}_1 - c_3 T_0, \\ A_{23}(e^{-s}) &= 0, \\ A_{31}(e^{-s}) &= c_3 C_{A,0} - c_3 C_{A,0} e^{-\rho s} = c_3 C_{A,0} \eta(\rho, s), \\ A_{32}(e^{-s}) &= c_3 T_0 - c_3 T_0 e^{-\rho s} = c_3 T_0 \eta(\rho, s), \\ A_{33}(e^{-s}) &= 0, \end{aligned}$$

where we let $\eta(\rho, s) = 1 - e^{-\rho s}$. Expanding this determinant, we obtain the following characteristic equation:

$$p_0(\rho, s) + p_1(\rho, s)e^{-\sigma s} + p_2(\rho, s)e^{-\tilde{\tau} s} + p_3(\rho, s)e^{-\tilde{\upsilon} s} = 0, \tag{9}$$

where

$$\begin{aligned} p_0(\rho, s) &= -s^3 + (-\tilde{b}_1 + \tilde{c}_1 - c_3 T_0)s^2 + (\tilde{b}_1\tilde{c}_1 - b_1 c_3 T_0 - b_2 c_3 C_{D,0} T_0)s \\ &\quad - (b_2 c_3 C_{A,0} T_0)s\eta(\rho, s) + (b_2\tilde{c}_1 c_3 C_{A,0} T_0)\eta(\rho, s), \\ p_1(\rho, s) &= b_3 C_{A,0} p_{\rho,\text{aux}}(s), \\ p_2(\rho, s) &= b_4 C_{A,0} p_{\rho,\text{aux}}(s), \\ p_3(\rho, s) &= b_5 C_{A,0} p_{\rho,\text{aux}}(s), \end{aligned}$$

for

$$p_{\rho,\text{aux}}(s) = (1 + \rho c_3)s^2 + (\rho c_3^2 T_0 - \tilde{c}_1(1 + \rho c_3))s + (c_3 T_0)s\eta(\rho, s) - (\tilde{c}_1 c_3 T_0)\eta(\rho, s).$$

3. **Main results.** One way of visualizing the crossing surface of (8) is to fix two delays and determine the crossing curves for the other two delays. Based on the particular form of the characteristic equation, it seems reasonable to first fix ρ. In addition, based on the delay scale, we will refer to the delays ρ and σ as *small* and the delays $\tilde{\tau}$ and $\tilde{\upsilon}$ as *large*.

We now fix ρ, and introduce an *auxiliary system* that is associated with the small delay σ, and is given by the following characteristic equation:

$$p_{\rho,\sigma}(s) = p_0(\rho, s) + p_1(\rho, s)e^{-\sigma s}. \tag{10}$$

Using the method presented in Section 4.2, we can easily determine the range of values of ρ that could result in stable systems. After finding the stable interval for ρ, we can easily characterize the *stability crossing curves* of $p_{\rho,\sigma}(s)$ given by (10) in the delay-parameter space defined by the small delays ρ, and σ. Based on such a characterization, and using a standard continuity argument (see, for instance, [14]) of the roots of the characteristic equation (9) with respect to the delay parameters, we make the following assumption:

Assumption 1. Let $\mathcal{I}_\rho \subset \mathbb{R}_+$, and $\mathcal{I}_\sigma \subset \mathbb{R}_+$ be some real intervals such that there exists some $\delta > 0$, such that $p_{\rho,\sigma}(s) \neq 0$ for all the pairs $(\sigma, \rho) \in \mathcal{I}_\sigma \times \mathcal{I}_\rho$, and for all $s \in \mathcal{V}_\delta$, where $\mathcal{V}_\delta$ is defined by:

$$\mathcal{V}_\delta \quad = \quad \{s \in \mathbb{C} : \quad -\delta < Re(s) < \delta\}. \tag{11}$$

This assumption above can be seen as a *regularity* condition for the original linearized model. It means that there exists some delay intervals such that $p_{\rho,\sigma}$ is *invertible* in some neighborhood $\mathcal{V}_\delta$ of the imaginary axis for all the pairs $(\sigma, \rho) \in \mathcal{I}_\sigma \times \mathcal{I}_\rho$.

It is important to note that the assumption above is not restrictive.

Indeed, assume now that there exists at least one root on the imaginary axis for the auxiliary characteristic equation $p_{\rho,\sigma}(s) = 0$. First, the number of roots on the imaginary axis of $p_{\rho,\sigma}(s) = 0$ is always *finite* (see the arguments in [19]). Next, if $j\omega_c \neq 0$ is one of such roots of the auxiliary characteristic equation $p_{\rho,\sigma}(j\omega_c) = 0$, then it is also a root of (9) *if and only if* the following modulus condition is satisfied:

$$| p_2(\rho, j\omega_c) | \quad = \quad | p_3(\rho, j\omega_c) |.$$

Then the crossing curve corresponding to the frequency $j\omega_c$ in the parameter space defined by the large delay values is given by the following argument condition:

$$p_2(\rho, j\omega_c) \quad = \quad p_3(\rho, j\omega_c)e^{-j(\pi+\omega_c(\tilde{\upsilon}-\tilde{\tau}))},$$

which lead to the definition of some equidistant lines in the delay parameter space $(\tilde{\tau}, \tilde{\upsilon})$.

Finally, if $j\omega_c$ does not satisfy the modulus condition above, then the regularity condition $p_{\rho,\sigma}(s) \neq 0$ is *still* valid on some interval on the imaginary axis $\mathcal{I}_\omega$, such that $j\omega_c \notin \mathcal{I}_\omega$. In such a case, Assumption 1 will be appropriately rewritten with respect to the corresponding imaginary axis interval. For the sake of brevity, such cases will not be considered in the paper. However, we point out that the corresponding analysis can be done in a similar manner.

3.1. **Identification of the crossing points, and crossing set characterization.** Since we assume that ρ is fixed, to simplify notation, we will write $p_2(s)$ and $p_3(s)$ instead of $p_2(\rho, s)$ and $p_3(\rho, s)$. We have the following result:

Proposition 1. *Assume that the auxiliary system given by (10) satisfies Assumption 1. Define*

$$a_{\tilde{\tau},\tilde{\upsilon}}(s) = 1 + a_{\tilde{\tau}}(s)e^{-s\tilde{\tau}} + a_{\tilde{\upsilon}}(s)e^{-s\tilde{\upsilon}}, \tag{12}$$

where $a_{\tilde{\tau}}(s) = \dfrac{p_3(s)}{p_{\rho,\sigma}(s)}$ *and* $a_{\tilde{\upsilon}}(s) = \dfrac{p_4(s)}{p_{\rho,\sigma}(s)}$, *for all* $(\sigma, \rho) \in \mathcal{I}_\sigma \times \mathcal{I}_\rho$. *Then for any* $(\sigma, \rho) \in \mathcal{I}_\sigma \times \mathcal{I}_\rho$, *the characteristic equation associated with (9) and* $a_{\tilde{\tau},\tilde{\upsilon}}(s)$ *have the same solutions in a neighborhood* $\mathcal{V}_\delta$ *of the imaginary axis, where:*

$$\mathcal{V}_\delta = \{s \in \mathbb{C} : \quad \delta \geq Re(s) > -\delta\},$$

for some $\delta > 0$.

Proof. The proof follows from the continuity argument with respect to the delay parameters (see, e.g. [14]), and from the equivalence between the characteristic equations (12) and (9) if $a_{\rho,\sigma}(s) \neq 0$ in some vertical strip including the imaginary axis (Assumption 1). □

3.2. **Weak T/C interactions, and delay-independence type results.** As mentioned in the Introduction, we will consider first the case of *weak T/C cell interactions*. Without any loss of generality, a weak T/C interaction simply means a reduced probability of interactions of anti-cancer and cancer cells. In other words, the weak T/C interaction describes the situations when the anti-cancer cells will tend to "ignore" the cancer cells.

Roughly speaking, such a T/C interaction will be translated in "small" values for the coefficients $b_4 = 2^N p_1 q_1 k$, and $b_5 = p_1 q_2 k$, which may correspond to the case when *no crossing* in the delay-parameter space defined by large delays exists. In conclusion, a weak T/C interaction may correspond to some *delay-independent* type property with respect to the delay parameters under consideration, and the last argument will give a way to define a *measure* for characterizing the interaction character.

With the notations, and the results above, we have the following:

Proposition 2 (Delay-independence in large delays)**.** *Assume that the auxiliary system given by the characteristic equation (10) satisfies the Assumption 1, and that* $a_{\tilde{\tau},\tilde{\upsilon}}(0) \neq 0$, *where* $a_{\tilde{\tau},\tilde{\upsilon}}$ *is defined by (12). Then the following statements are equivalent:*

(a) *If the auxiliary system (10) is stable for some pair* $(\rho, \sigma) \in \mathcal{I}_\rho \times \mathcal{I}_\sigma$, *and if the system free of delays* ($\sigma = \rho = \tilde{\tau} = \tilde{\upsilon} \equiv 0$) *given by (8) when all delays are set to* 0 *is stable, then the system (5) is stable for all pairs* $(\tilde{\tau}, \tilde{\upsilon}) \in \mathbb{R}_+ \times \mathbb{R}_+$, *and there does not exist any root crossing the imaginary axis when the delays* $\tilde{\tau}$, *and* $\tilde{\upsilon}$ *are increased in* $\mathbb{R}_+$.

(b) *The following frequency-sweeping test holds:*

$$\frac{\mid C_{A,0} \mid\mid p_{\rho,aux}(j\omega) \mid}{\mid p_{\rho,\sigma}(j\omega) \mid} < \frac{1}{(2^N q_1 + q_2) p_1 k}, \quad \forall \omega > 0. \tag{13}$$

The same equivalence holds if the stability property is replaced by the instability of the system with a prescribed number of unstable roots.

Proof. It is easy to see that the condition (13) is equivalent to the condition $a_{\tilde{\tau},\tilde{\upsilon}}(j\omega) \neq 0$, for all $\omega > 0$. Then the equivalence between conditions *(a)* and *(b)* above follows straightforwardly since $a_{\tilde{\tau},\tilde{\upsilon}} \neq 0$ whenever $\omega = 0$, and thus $a_{\tilde{\tau},\tilde{\upsilon}} \neq 0$ on the whole imaginary axis. Next, no crossing with respect to the imaginary axis means that the stability property valid for $\tilde{\tau} = \tilde{\upsilon} = 0$ is valid for all $(\tilde{\tau}, \tilde{\upsilon}) \in \mathbb{R}_+ \times \mathbb{R}_+$ (see, for instance, the arguments in [18, 31] for delay-independent stability characterization). The instability property follows similarly (see, for instance, the discussions on hyperbolicity in [31, 21]). □

In other words, the result above gives a simple test for describing the situations when the system (5), *stable* or *unstable* in the case when is *delay-free*, will remain *stable* or respectively *unstable* for *all positive (large) delays* $\tilde{\tau}$, and $\tilde{\upsilon}$.

Remark 1. (delay-independent/delay-dependent) The main difference between the result above, and the standard *delay-independent* frequency-sweeping tests (see, e.g. [18]) is the fact that, in our case, we do not impose the delay-independent property with respect to the *whole* set of delays, ρ, σ, $\tilde{\upsilon}$, and $\tilde{\tau}$; rather, it is delay-independent with respect to a subset of delays, $\tilde{\tau}$ and $\tilde{\upsilon}$.

Several remarks about "mixed" delay-independent/delay-dependent stability results can be found in [31]. Furthermore, the *delay-independent* character can be seen as the existence of at least one *unbounded* direction in the corresponding delay-parameter set. Such a problem was considered by [20] in the particular case of a scalar system including two discrete delays.

Remark 2 (Weak T/C interaction measure)**.** The frequency-sweeping test (13) can be used to define a measure for characterizing the T/C interaction type in the following sense: the T/C interaction will be called *weak* if the probabilities (q_1, q_2), and the average number of cell division N verify the condition:

$$2^N q_1 + q_2 < \frac{1}{p_1 k} \cdot \frac{1}{\sup_{\omega \in \mathbb{R}} \frac{|C_{A,0}||p_{\rho,\mathrm{aux}}(j\omega)|}{|p_{\rho,\sigma}(j\omega)|}}. \tag{14}$$

The condition (14) gives the corresponding *T/C interaction measure*. It becomes clear that the average number N of cell division plays a central role in defining the T/C interaction character, since the quantity $2^N q_1 + q_2$ is an increasing function of N.

Remark 3 (Delay-independence in three delays)**.** For all three delays σ, $\tilde{\tau}$, and $\tilde{\upsilon}$, the frequency-sweeping test is

$$\frac{\mid C_{A,0} \mid\mid p_{\rho,\mathrm{aux}}(j\omega) \mid}{\mid p_{\rho,\sigma}(j\omega) \mid} < \frac{1}{\mid b_3 \mid + \mid b_4 \mid + \mid b_5 \mid} = \frac{1}{k(p_2 + p_1(2^N q_1 + q_2))}, \quad \forall \omega > 0. \tag{15}$$

This relation can be derived in the same manner as (13).

3.3. **Strong T/C interactions, and identification of the crossing points.** As mentioned in the previous paragraph, the existence of crossing sets in the delay-parameter space defined by $\tilde{\tau}$ and $\tilde{\upsilon}$ is related to the fact that the inequality (13) is not verified for all $\omega > 0$, or in other words that the parameters (q_1, q_2, N) do not satisfy the measure condition (14) for the T/C weak interaction.

Let us characterize now the strong T/C interactions. Inspired by the work in [19], the condition that $a_{\tilde{\tau},\tilde{\upsilon}}$ defined by (12) has at least one root $j\omega_0$ on the imaginary axis is reduced geometrically to the condition that the "lengths" 1, $\mid a_\upsilon(j\omega_0) \mid$, and $\mid a_\mu(j\omega_0) \mid$ define a triangle. Thus, some simple computations lead to the following criterion for the *identification of the crossing points*:

Proposition 3. *Assume that the auxiliary system given by the characteristic equation (10) satisfies the Assumption 1. Then each $\omega \in \mathbb{R}_+$ can be a solution of the characteristic equation associated to Σ for some $(\tilde{\tau}, \tilde{\upsilon}) \in \mathbb{R}_+^2$ if and only if:*

$$\frac{1}{(2^N q_1 + q_2)p_1 k} \leq \frac{\mid C_{A,0} \mid\mid p_{\rho,aux}(j\omega) \mid}{\mid p_{\rho,\sigma}(j\omega) \mid} \leq \frac{1}{\mid 2^N q_1 - q_2 \mid p_1 k}. \tag{16}$$

Then, the *crossing set* Ω will be defined by all $\omega \in \mathbb{R}_+$, for which the frequency condition (16) holds. In conclusion, the algorithm for identifying the crossing points can be summarized as follows:

- first, we represent graphically $\dfrac{\mid C_{A,0} \mid\mid p_{\rho,\mathrm{aux}}(j\omega) \mid}{\mid p_{\rho,\sigma}(j\omega) \mid}$ against ω, and
- next we analyze the intersection of this graph with two parallel lines to ω-axis: $1/((2^N q_1 + q_2)p_1 k)$ and $1/(\mid 2^N q_1 - q_2 \mid p_1 k)$, respectively.

Let $\omega \in \Omega$ be a crossing point. Then from the triangle geometry it follows that:

$$\tilde{\tau} = \tilde{\tau}^{u\pm}(\omega) = \frac{\angle a_{\tilde{\tau}}(j\omega) + (2u-1)\pi \pm \theta_1}{\omega} \geq 0, \quad \text{for } u = u_0^{\pm}, u_0^{\pm} + 1, u_0^{\pm} + 2, ..., \tag{17}$$

$$\tilde{\upsilon} = \tilde{\upsilon}^{v\pm}(\omega) = \frac{\angle a_{\tilde{\upsilon}}(j\omega) + (2v-1)\pi \mp \theta_2}{\omega} \geq 0, \quad \text{for } v = v_0^{\pm}, v_0^{\pm} + 1, v_0^{\pm} + 2, ..., \tag{18}$$

where $\theta_1, \theta_2 \in [0, \pi]$ are the internal angles of the triangle formed by the lengths 1, $\mid a_{\tilde{\tau}} \mid$, and $\mid a_{\tilde{\upsilon}} \mid$, and can be calculated by the law of cosine as

$$\theta_1 = \cos^{-1}\left(\frac{1 + |a_{\tilde{\tau}}(j\omega)|^2 - |a_{\tilde{\upsilon}}(j\omega)|^2}{2|a_{\tilde{\tau}}(j\omega)|}\right), \tag{19}$$

$$\theta_2 = \cos^{-1}\left(\frac{1 + |a_{\tilde{\upsilon}}(j\omega)|^2 - |a_{\tilde{\tau}}(j\omega)|^2}{2|a_{\tilde{\upsilon}}(j\omega)|}\right), \tag{20}$$

and u_0^+, u_0^-, v_0^+, v_0^- are the smallest possible integers (may be negative and may depend on ω) such that the corresponding $\tilde{\tau}^{u_0^+ +}$, $\tilde{\tau}^{u_0^- -}$, $\tilde{\upsilon}^{v_0^+ +}$, $\tilde{\upsilon}^{v_0^- -}$ are nonnegative.

Let $\mathcal{T}^{+}_{\omega,u,v}$ and $\mathcal{T}^{-}_{\omega,u,v}$ be the singletons defined by

$$\mathcal{T}^{\pm}_{\omega,u,v} = \{(\tilde{\tau}^{u\pm}(\omega), \tilde{v}^{v\pm}(\omega))\},$$

and define

$$\mathcal{T}_{\omega} = \left(\bigcup_{\substack{u\geq u_0^{+} \\ v\geq v_0^{+}}} \mathcal{T}^{+}_{\omega,u,v} \right) \bigcup \left(\bigcup_{\substack{u\geq u_0^{-} \\ v\geq v_0^{-}}} \mathcal{T}^{-}_{\omega,u,v} \right).$$

Then $\mathcal{T}_{\omega}$ is the set of all $(\tilde{\tau}, \tilde{v})$ such that $a_{\tilde{\tau},\tilde{v}}$ has one zero at $s = j\omega$.

Remark 4. It is easy to see that $\dfrac{\mid C_0 \mid \sqrt{\tilde{c}_1^2 + \omega^2}}{\mid p_{\rho,\sigma}(j\omega) \mid} \to 0$, when $\omega \to +\infty$, and in conclusion $\infty \notin \Omega$. In other words, Ω is *bounded*.

In [19], the characterization of the stability crossing curves for a general system including *two delays* was based on an important property of the corresponding *stability crossing set*. More precisely, such a set consisted of a finite number of intervals of finite length. In our case, in order to completely characterize the crossing curves in the parameter space defined by the large delays, it is interesting to have a similar property. The fact that Ω is *bounded* was proved in the last remark above.

Assumption 2. The following condition holds:

$$\frac{d}{d\omega}\left(\frac{\mid C_{A,0} \mid\mid p_{\rho,\text{aux}}(j\omega) \mid}{\mid p_{\rho,\sigma}(j\omega) \mid} \right) \neq 0 \text{ whenever } h(\omega) = \frac{1}{\mid 2^N q_1 \pm q_2 \mid p_1 k}.$$

This assumption simply requires that the corresponding differentiable function satisfies some non-degenerate property at the corresponding upper, and lower bounds given by (16).

With the remarks and the assumptions above, we have:

Proposition 4. *Under Assumptions 1 and 2, the crossing set Ω consists of a finite number of intervals of finite length.*

Proof. Define the function $h : \mathbb{R}_+ \mapsto \mathbb{R}_+$ by:

$$h(\omega) := \frac{\mid C_{A,0} \mid\mid p_{\rho,\text{aux}}(j\omega) \mid}{\mid p_{\rho,\sigma}(j\omega) \mid}. \tag{21}$$

Thus, the condition (16) defining the crossing set Ω rewrites as:

$$\frac{1}{(2^N q_1 + q_2) p_1 k} \leq h(\omega) \leq \frac{1}{\mid 2^N q_1 - q_2 \mid p_1 k}.$$

Since Ω is bounded (see Remark 4), it is sufficient to prove that $h(\omega) = \frac{1}{(2^N q_1 \pm q_2) p_1 k}$ has a finite number of solutions in $[0, \omega_{max}]$, where $\omega_{max} = \sup\{\omega | \omega \in \Omega\}$. This will be shown by contradiction.

Assume, for example, that $h(\omega) = \frac{1}{(2^N q_1 + q_2) p_1 k}$ has an *infinite* number of solutions ω_i, $i = 1, 2, \ldots$, with $[0, \omega_{max}]$. Then

$$h(\omega_i) = \frac{1}{(2^N q_1 + q_2) p_1 k}, \quad \omega_i \in [0, \omega_{max}], \quad i = 1, 2, \ldots$$

In such a case, there exists a sub-series i_m such that

$$\lim_{i_m \to \infty} \omega_{i_m} = \omega_0.$$

But this last condition simply means:

$$\frac{d}{d\omega}h(\omega) = \lim_{i_m \to \infty} \frac{h(\omega_{i_m}) - h(\omega_0)}{\omega_{i_m} - \omega_0} = 0,$$

contradicting Assumption 2. □

3.4. **Characterization of the crossing curves.** The next step is to characterize the crossing curves of the system (5), or equivalently all the crossing curves satisfying $a_{\tilde{\tau},\tilde{\upsilon}}(s) = 0$ for $s = j\omega$, $\omega \in \Omega$.

Using an argument similar to the one developed by [19] (type classification of the crossing points), define by $\Omega_k \subset \Omega$ some interval of crossing set Ω, and let $\mathcal{T}^k \subset \mathcal{T}$ be the corresponding stability crossing curves for some positive integer k, we have the following:

Proposition 5. *Under Assumptions 1 and 2, the stability crossing curves $\mathcal{T}^k$ corresponding to Ω_k must be an intersection of $\mathbb{R}^2_+$ with a series of curves belonging to one of the following categories:*

A. A series of closed curves;
B. A series of spiral-like curves with axes oriented either horizontally, vertically, or diagonally.
C. A series of open ended curves with both ends approaching ∞.

Remark 5. The classification above is given by the way the end points of the corresponding intervals Ω_k are derived.

3.5. **Tangent and smoothness.** In this section, for a given k, we will discuss the smoothness of the curves in $\mathcal{T}^k$ and thus $\mathcal{T} = \bigcup_{k=1}^{N} \mathcal{T}^k$. We will assume that a k is given and will refer to $\mathcal{T}^k$ without further comments. In addition to the explicit formulas (17) and (18), we will also use an approach similar to the one described in Chapter 11 of [16] based on the implicit function theorem.

For this purpose, we consider $\tilde{\tau}$ and $\tilde{\upsilon}$ as implicit functions of $s = j\omega$ defined by $a_{\tilde{\tau},\tilde{\upsilon}} = 0$. As s moves along the imaginary axis, $(\tilde{\tau}, \tilde{\upsilon}) = (\tilde{\tau}^{u\pm}(\omega), \tilde{\upsilon}^{v\pm}(\omega))$ moves along $\mathcal{T}^k$. For a given $\omega \in \Omega_k$, let

$$\begin{aligned} R_0 &= Re\left(\frac{j}{s}\frac{\partial a_{\tilde{\tau},\tilde{\upsilon}}(s)}{\partial s}\right)_{s=j\omega} \\ &= \frac{1}{\omega} Re\left(\left[a'_{\tilde{\tau}}(j\omega) - \tilde{\tau}a_{\tilde{\tau}}(j\omega)\right] e^{-j\tilde{\tau}\omega} + \left[a'_{\tilde{\upsilon}}(j\omega) - \tilde{\upsilon}a_{\tilde{\upsilon}}(j\omega)\right]e^{-j\tilde{\upsilon}\omega}\right), \end{aligned} \tag{22}$$

$$\begin{aligned} I_0 &= Im\left(\frac{j}{s}\frac{\partial a_{\tilde{\tau},\tilde{\upsilon}}(s)}{\partial s}\right)_{s=j\omega} \\ &= \frac{1}{\omega} Im\left(\left[a'_{\tilde{\tau}}(j\omega) - \tilde{\tau}a_{\tilde{\tau}}(j\omega)\right] e^{-j\tilde{\tau}\omega} + \left[a'_{\tilde{\upsilon}}(j\omega) - \tilde{\upsilon}a_{\tilde{\upsilon}}(j\omega)\right]e^{-j\tilde{\upsilon}\omega}\right), \end{aligned} \tag{23}$$

and

$$R_l = -Re\left(\frac{1}{s}\frac{\partial a_{\tilde{\tau},\tilde{\upsilon}}(s))}{\partial \tau_k}\right)_{s=j\omega}, \tag{24}$$

$$I_l = -Im\left(\frac{1}{s}\frac{\partial a_{\tilde{\tau},\tilde{\upsilon}}(s)}{\partial \tau_k}\right)_{s=j\omega}, \tag{25}$$

for $l = 1, 2$, and τ_1, τ_2 correspond to $\tilde{\tau}$, and $\tilde{v}$, respectively. Then, since $a_{\tilde{\tau},\tilde{v}}(s)$ is an analytic function of s, $\tilde{\tau}$ and $\tilde{v}$, the implicit function theorem indicates that the tangent of $\mathcal{T}^k$ can be expressed as

$$\begin{pmatrix} \frac{d\mu}{d\omega} \\ \frac{dv}{d\omega} \end{pmatrix} = \begin{pmatrix} R_1 & R_2 \\ I_1 & I_2 \end{pmatrix}^{-1} \begin{pmatrix} R_0 \\ I_0 \end{pmatrix} = \frac{1}{R_1 I_2 - R_2 I_1} \begin{pmatrix} R_0 I_2 - I_0 R_2 \\ I_0 R_1 - R_0 I_1 \end{pmatrix}, \tag{26}$$

provided that

$$R_1 I_2 - R_2 I_1 \neq 0. \tag{27}$$

It follows from a well known result [8] that $\mathcal{T}^k$ is smooth everywhere except possibly at the points where either (27) is not satisfied, or when

$$\frac{d\tilde{\tau}}{d\omega} = \frac{d\tilde{v}}{d\omega} = 0. \tag{28}$$

A careful examination of these cases allows us to conclude the following:

Proposition 6. *Under Assumption 1, the curves in $\mathcal{T}^k$ are smooth everywhere except possibly at the degenerate points corresponding to ω in any one of the following two cases:*

Case 1. $s = j\omega$ is a multiple solution of $a_{\tilde{\tau},\tilde{v}}(j\omega) = 0$.

Case 2. ω is an end point, and

$$\frac{d}{d\omega}\left(\frac{|\, C_0 \,| \sqrt{\tilde{c}_1^2 + \omega^2}}{|\, p_{\rho,\sigma}(j\omega) \,|}\right) = 0.$$

3.6. **Direction of crossing.** Next, we will discuss the direction in which the solutions of the characteristic equation given by $a_{\tilde{\tau},\tilde{v}}(s) = 0$ cross the imaginary axis as $(\tilde{\tau}, \tilde{v})$ deviates from a curve in $\mathcal{T}^k$. We will call the direction of the curve that corresponds to increasing ω the *positive direction*. Notice, as the curve passes through the points corresponding to the end points of Ω_k, the positive direction is reversed. We will also call the region on the left hand side as we head in the positive direction of the curve *the region on the left*. Again, due to the possible reversal of parameterization, the same region may be considered on the left with respect to one point of the curve, and be considered as on the right on another point of the curve.

For the purpose of discussing the direction of crossing, we need to consider $\tilde{\tau}$ and $\tilde{v}$ as functions of $s = r + j\omega$, i.e., functions of two real variables r and ω, and partial derivative notation needs to be adopted instead. Since the tangent of $\mathcal{T}^k$ along the positive direction is $(\partial\tilde{\tau}/\partial\omega, \partial\tilde{v}/\partial\omega)$, the normal to $\mathcal{T}^k$ pointing to the left hand side of the positive direction is $(-\partial\tilde{v}/\partial\omega, \partial\tilde{\tau}/\partial\omega)$. Also, as a pair of complex conjugate solutions of $a_{\tilde{\tau},\tilde{v}} = 0$ cross the imaginary axis to the $\mathbb{C}_+$, $(\tilde{\tau}, \tilde{v})$ move along the direction $(\partial\tilde{\tau}/\partial r, \partial\tilde{v}/\partial r)$. We can therefore conclude that if the inner product of these two vectors are positive, i.e.,

$$\left[\frac{\partial\tilde{\tau}}{\partial\omega}\frac{\partial\tilde{v}}{\partial r} - \frac{\partial\tilde{v}}{\partial\omega}\frac{\partial\tilde{\tau}}{\partial r}\right]_{s=j\omega} > 0, \tag{29}$$

the region on the left of $\mathcal{T}^k$ at ω has two more solutions in $\mathbb{C}_+$. On the other hand, if the inequality in (29) is reversed, then the region on the left of $\mathcal{T}^k$ has two fewer solutions on the right hand side of the complex plane. We can very easily express,

parallel to (26), that,

$$\begin{pmatrix} \frac{\partial \tilde{\tau}}{\partial r} \\ \frac{\partial \tilde{\upsilon}}{\partial r} \end{pmatrix}_{s=j\omega} = \begin{pmatrix} R_1 & R_2 \\ I_1 & I_2 \end{pmatrix}^{-1} \begin{pmatrix} I_0 \\ -R_0 \end{pmatrix} = \frac{1}{R_1 I_2 - R_2 I_1} \begin{pmatrix} R_0 R_2 + I_0 I_2 \\ -R_0 R_1 - I_0 I_1 \end{pmatrix}, \tag{30}$$

where R_l and I_l, $l = 0, 1, 2$, are defined in (22) to (25). This allows us to arrive at the following proposition.

Proposition 7. *Let $\omega \in \Omega_k$, but an end point, and $(\tilde{\tau}, \tilde{\upsilon}) \in \mathcal{T}^k$ such that $j\omega$ is a simple solution of $a_{\tilde{\tau},\tilde{\upsilon}}(s) = 0$, and*

$$a_{\tilde{\tau},\tilde{\upsilon}}(j\omega') \neq 0, \text{ for any } \omega' > 0,\ \omega' \neq \omega. \tag{31}$$

Then as $(\tilde{\tau}, \tilde{\upsilon})$ moves from the region on the right to the the region on the left of the corresponding curve in $\mathcal{T}^k$, a pair of solutions of $a_{\tilde{\tau},\tilde{\upsilon}}(s) = 0$ cross the imaginary axis to the right if

$$R_2 I_1 - R_1 I_2 > 0. \tag{32}$$

4. **Illustrative example.** In this section, we show how the techniques developed in Sections 3 and 4 can be used to study the stability of (1) with respect to delays. The analysis is completed with a discussion of the results.

4.1. **Stability without delays.** For our application in [15], we estimated the parameters to be

$$\begin{array}{lll} d_T = 0.2, & p_1 = 0.5, & \rho = 0.0035, \\ r = 0.2, & p_2 = 0.5, & \sigma = 0.0007, \\ k = 1, & q_1 = 0.5, & \tilde{\tau} = 2.0035, \\ N = 2, & q_2 = 0.5, & \tilde{\upsilon} = 1.0035. \\ K = 200, & \tilde{p}_1 = 0.5, & \end{array} \tag{33}$$

Hence, b_1, c_1, and b are of order 1 or 0.1.

Fixed point 1: $(T_0, C_{A,0}, C_{D,0}) = (0, 0, 0)$

For the fixed point $(T_0, C_{A,0}, C_{D,0}) = (0, 0, 0)$, the characteristic equation given by (9) is

$$0 = s^3 + (\tilde{b}_1 - \tilde{c}_1)s^2 - \tilde{b}_1\tilde{c}_1 s = s(s^2 + (b_1 - c_1)s - b_1 c_1),$$

regardless of the delays. Substituting the parameters from (33), we obtain

$$s(s^2 - 0.04) = 0,$$

which has roots -0.2, 0, and 0.2. Note that due to the format of the equation and the assumption that all parameters are positive. This characteristic equation is always unstable, even with other biologically relevant parameters.

Fixed point 2: $(T_0, C_{A,0}, C_{D,0}) = (0, K, 0)$

In the case where all delays are set to 0 and the parameters from (33) are used, we obtain the fixed point $(T_0, C_{A,0}, C_{D,0}) = (0, 200, 0)$. Then, the characteristic equation given by (9) is

$$s^3 - 149.6s^2 - 29.96s = s(s^2 - 149.6s - 29.96) = 0,$$

which has roots -149.8, 0, and 0.2. Hence, this fixed point is unstable when all delays are set to 0.

Fixed point 3: The fixed point $(T_0, C_{A,0}, C_{D,0})$ is determined by (6) and (7).

When non-delay parameter values from (33) are used, the equation (6) for T_0 is

$$0.1875\rho T_0^2 + (0.375 - 0.075\rho)T_0 - 0.1498 = 0.$$

Since the constant term is negative, the equation yields only one positive solution for T_0, which means only one biologically feasible fixed point exists.

In the case where all delays are set to 0, we obtain $T_0 = 0.3995$, and from (7), we obtain $C_{A,0} = 0.2667$ and $C_{D,0} = 0$. Thus, from (9), we obtain the characteristic equation

$$s(s^2 + 2.4333 \times 10^{-4}s + 3.9947 \times 10^{-2}) = 0,$$

which has roots 0 and $-0.0001 \pm 0.1999j$. Hence, the linearized system is marginally stable when all delays are set to 0.

Proposition 8. *The fixed points of the linearized system without delay have the following properties:*

(a) The fixed-point FP-I $(T_0, C_0) = (0, 0, 0)$ is a saddle.
(b) The fixed point FP-II $(T_0, C_0) = (0, K, 0)$ is a saddle.
(c) The fixed point FP-III, determined by (6) and (7), has two stable eigenvalues and one eigenvalue at 0.

Proof. (a) As mentioned above, FP–I is a saddle independent of the parameter choice. (b) Next, in our case, the computation shown above proves that the fixed point FP–II is a saddle. (c) Finally, for the parameters in the vicinity of (33), the solution at FP–III, which represents a controlled disease state, has its rightmost eigenvalue at 0. Since the system is nonlinear, it requires further analysis to determine the stability of this fixed point. □

It is clear that FP–III is of *most interest* to us because it represents the case where the immune response controls the cancer population. However, since the characteristic equation of this fixed point has an eigenvalue at 0 and two eigenvalues with very small real part (on the order of -10^{-4}), the approach to the fixed point is, at best, very slow. In fact, the stability of the fixed point is so low that numerical error may cause the solution to become unstable. When solving DDEs in Matlab, one way around this problem is to increase the relative and absolute tolerances of the MATLAB DDE solver.

4.2. **Stability of FP–III with delays.** In the following sections we will perform a more thorough analysis of the eigenvalues of the characteristic equation (9) for FP–III with respect to the delay values. As stated in Proposition 8, the characteristic equation for FP–III has two conjugate eigenvalues with real part less than 0 and one eigenvalue at 0.

In fact, the system has a 0 eigenvalue no matter what the four delays are. The zero eigenvalue is due to the description of the dying cancer cell population. Indeed, a close inspection of the equation for C_D in (1) indicates that an initial condition with positive C_D and zero C_A and T results in a permanently positive population of dying cells. However, in practice, this type of disturbance is not present due to the fact that all dying cells have a finite life span, ρ. Therefore, the mode corresponding

to the zero eigenvalue can be easily separated from the rest of the system. Indeed, we may replace the third differential equation of (1) by the equivalent integral equation (modulo a constant), i.e.,

$$C_D(t) = \tilde{p_1} k \int_{-\rho}^{0} C_A(t+w)T(t+w)dw,$$

which will eliminate the mode with the zero eigenvalue. Hence, we study the behavior of the other eigenvalues excluding the fixed eigenvalue at 0, so we consider the characteristic equation for $s > 0$.

If we set all delays to 0 except ρ, we obtain the following characteristic equation

$$\begin{aligned}
0 &= p_0(\rho, s) + p_1(\rho, s) + p_2(\rho, s) + p_3(\rho, s) \\
&= -s^3 + (-\tilde{b}_1 + \tilde{c}_1 - c_3T_0 + (b_3 + b_4 + b_5)C_{A,0}(1 + \rho c_3))s^2 \\
&\quad + \left[\tilde{b}_1\tilde{c}_1 - b_1c_3T_0 - b_2c_3C_{D,0}T_0 + (b_3 + b_4 + b_5)C_{A,0}(\rho c_3^2T_0 - \tilde{c}_1(1 + \rho c_3))\right] s \\
&\quad + bc_3C_{A,0}T_0(s - \tilde{c}_1) - bc_3C_{A,0}T_0(s - \tilde{c}_1)e^{-\rho s},
\end{aligned}$$

which is of the form

$$q_0(\rho, s) + q_1(\rho, s)e^{-\rho s} = 0, \tag{34}$$

where the coefficients of $q_0(\rho, s)$ and $q_1(\rho, s)$ depend on ρ. To locate stability crossings, we are interested in purely imaginary roots $s = j\omega$, and from the characteristic equation it follows that

$$\frac{q_0(\rho, j\omega)}{q_1(\rho, j\omega)} = 1. \tag{35}$$

Hence, we can implicitly express ω as a function of ρ.

Figure 3(a) shows a plot of ω as a function of ρ for $\rho \in [0, 1]$.

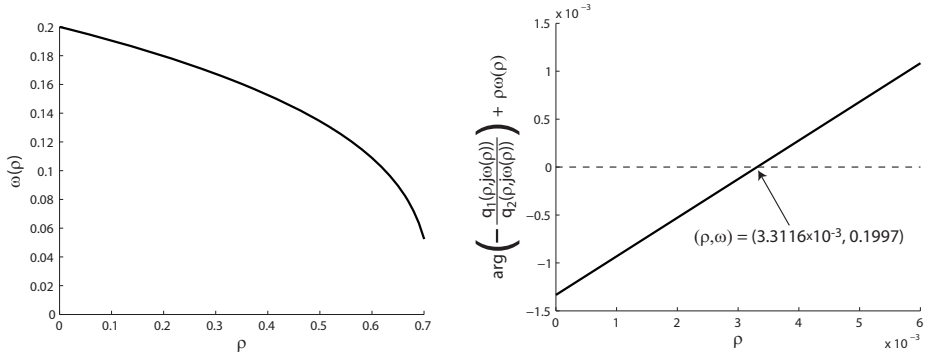

(a) **(b)**

FIGURE 3. (a) Graph of the stability crossing point $\omega(\rho)$ as a function of the time delay ρ based on the implicit relation (35). (b) Graph of $\arg\left(-\frac{q_0(\rho,j\omega(\rho))}{q_1(\rho,j\omega(\rho))}\right) + \rho\omega(\rho)$ as a function of ρ. We are interested in when the expression equals 0, thus satisfying (34).

Once we have ω as a function of ρ, we can use the equation

$$\arg\left(-\frac{q_0(\rho, j\omega(\rho))}{q_1(\rho, j\omega(\rho))}\right) + \rho\omega(\rho) = 0$$

to determine which values of ρ solve (34). Figure 3(b) shows a plot of $\arg\left(-\frac{q_0(\rho,j\omega(\rho))}{q_1(\rho,j\omega(\rho))}\right) + \rho\omega(\rho)$ as a function of ρ.

The value of ρ at which this expression equals 0 is $\rho = 3.3116\times10^{-3}$. Hence, other than the permanent root at 0, the system has stable eigenvalues for $\rho \in [0, 0.0033)$ when all other delays are set to 0. The boundary for instability is close to (and slightly less than) the estimated value of ρ which is 0.0035. To preserve stability, we reestimate the value of ρ to be 0.003 days (4.3 minutes).

From the above reasoning, we know that the system is stable (i.e. there are no roots with real part strictly greater than 0) when $\rho = 0.003$ and all the other delays are equal to 0.

4.3. **Crossing curves of the large delay $\tilde{\tau}$ versus the small delay σ.** As mentioned in Section 3, one way of visualizing the crossing surface of (8) is to fix two delays, in this case ρ and $\tilde{v}$, and determine the crossing curves for the other two delays, in this case σ and $\tilde{\tau}$.

In this section, we assume that $\rho = 0.003$ (and later 0.001). We then fix $\tilde{v} = 0$ and look at the crossing curves with respect to the small delay σ and the large delay $\tilde{\tau}$. Figure 4(a) shows the resulting crossing curves. As we see from Figure 4(a),

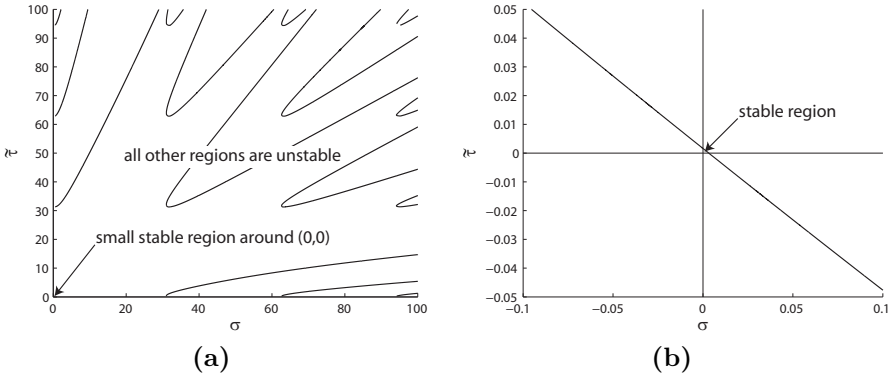

FIGURE 4. Crossing curves with respect to σ and $\tilde{\tau}$. (a) The zoomed-out plot shows the overall structure of the crossing curves for when $\rho = 0.003$ and $\tilde{v} = 0$. (b) The zoomed-in plot shows the small region of stability around the origin for when $\rho = 0.001$ and $\tilde{v} = 0$. Note that only nonnegative delays make sense.

the system is not stable for large σ and $\tilde{\tau}$. There is a small stable region around $(0, 0)$. However, for $\rho = 0.003$, it nearly vanishes, and hence is hard to determine numerically. As a result, in Figure 4(b), we plot a close up view of the small stable region around the origin for $\rho = 0.001$. This small stable region quickly diminishes as ρ increases and completely vanishes when $\rho = 3.3116 \times 10^{-3}$ as discussed at the end of Section 4.2. Since sigma is a small delay (~ 0.0007), while $\tilde{\tau}$ is large (~ 2.0035), this small stable region may be relevant for σ, but is too small to be relevant for $\tilde{\tau}$.

For comparison, when $\rho = 0.001$ and $\tilde{v} = 0.005$, the stable region around the origin disappears, and the system is not stable for any (positive) choice of σ and $\tilde{\tau}$. Figure 5 shows that the stable region around $(0, 0)$ disappears when $\tilde{v} = 0.005$. From this figure, it is apparent that the stability of the system is sensitive to small

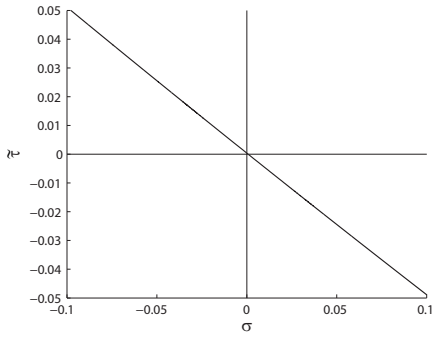

FIGURE 5. Crossing curves for σ and $\tilde{\tau}$ when $\rho = 0.001$ and $\tilde{\upsilon} = 0.005$. The stable region around the origin disappears for this value of $\tilde{\upsilon}$.

changes in the delay $\tilde{\upsilon}$.

However, it is interesting to note that around $\tilde{\upsilon} = 25$, the stable region around 0 reappears. The new stable region is also about two orders of magnitude larger, making it of relevant size to include reasonable values for $\tilde{\tau}$. Figure 6 shows crossing curves of σ vs. $\tilde{\tau}$ when $\tilde{\upsilon} = 25$. We will inspect this stable region again in Section 4.5.

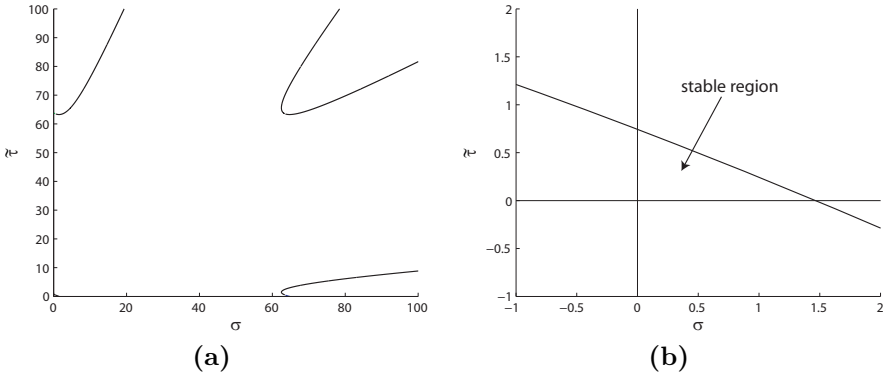

FIGURE 6. Crossing curves for σ and $\tilde{\tau}$ when $\rho = 0.003$ and $\tilde{\upsilon} = 25$. (a) The zoomed-out plot shows the overall structure of the crossing curves. (b) The zoomed-in plot shows the region of stability around the origin. The stability region around the origin is about two to three orders of magnitude larger than the one in Figure 4(b).

4.4. **Crossing curves of the large delays $\tilde{\tau}$ and $\tilde{\upsilon}$ versus the small delay σ.** In this section, we take $N = 1$ (i.e., we assume that T cells divide once upon stimulation by cancer cells) and assume that $\tilde{\tau} = \tilde{\upsilon}$. When $N = 1$, this assumption makes sense, since $\tilde{\tau} = \rho + N\tau$ and $\tilde{\upsilon} = \rho + \upsilon$, and both τ and υ are approximately equal to 1. (See (4) and Section 1.2.) In this case, the characteristic equation (9) can be rewritten as

$$p_0(\rho, s) + p_1(\rho, s)e^{-\sigma s} + (p_2(\rho, s) + p_3(\rho, s))e^{-\tilde{\tau} s} = 0,$$

and we can perform the stability analysis with respect to the two delays σ and $\tilde{\tau}$ $(= \tilde{v})$.

Figure 7 shows crossing curves for σ and the large delays ($\tilde{\tau}$ and $\tilde{v}$) when $\rho = 0.003$. As before, there is a small stable region around the origin.

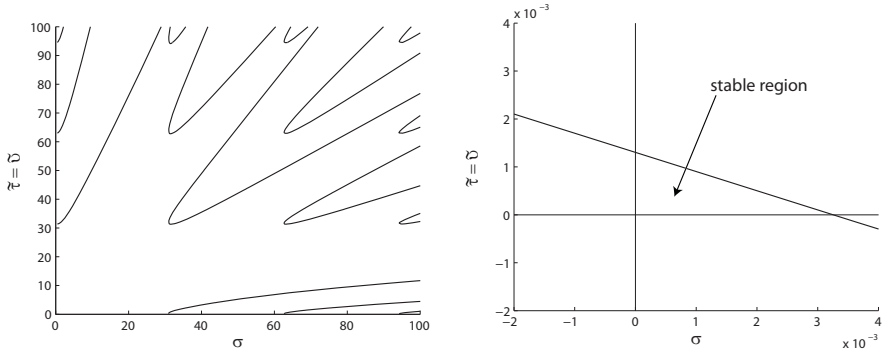

FIGURE 7. Set $N = 1$ and assume that $\tilde{\tau} = \tilde{v}$. Also, take $\rho = 0.003$. (a) The zoomed-out plot shows the overall structure of the crossing curves. (b) The zoomed-in plot shows the small region of stability around the origin. The stability region around the origin is comparable in size to the one in Figure 4(b).

4.5. **Crossing curves of the two large delays: $\tilde{v}$ vs. $\tilde{\tau}$.** We take $\rho = 0.001$ as done previously. We then fix σ and determine the crossing curves of $\tilde{v}$ vs. $\tilde{\tau}$. Figure 8 shows crossing curves when $\sigma = 0$ and $\sigma = 0.0007$. As before, there is a small stable region around the origin.

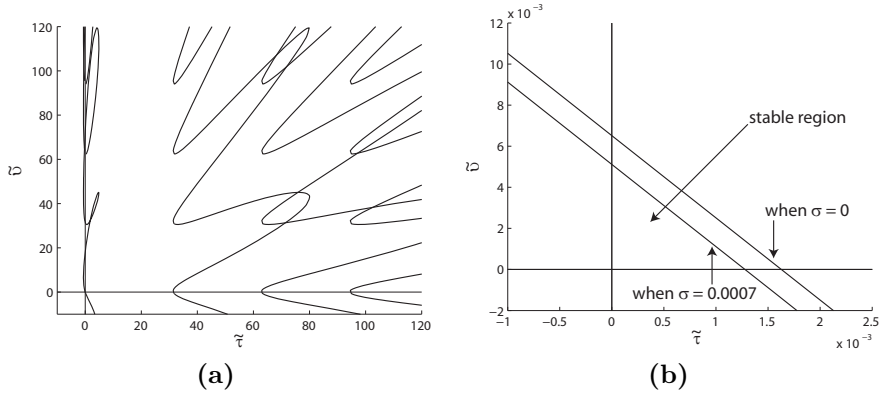

FIGURE 8. Crossing curves for $\tilde{\tau}$ and $\tilde{v}$ when $\rho = 0.001$. (a) The zoomed-out plot shows the crossing curves when $\sigma = 0$. The figure hardly changes when $\sigma = 0.0007$. (b) The zoomed-in plot shows the small stable regions near the origin when $\sigma = 0$ and $\sigma = 0.0007$. As shown in the figure, the stable region shrinks slightly as σ increases from 0 to 0.0007.

As remarked in Section 4.3 (Figure 6), there is another region of stability for large values of $\tilde{v}$. In Figure 9, we set $\rho = 0.001$ and $\sigma = 0.0007$, and plot the crossing curves with respect to $\tilde{\tau}$ and $\tilde{v}$. As shown in Figure 9(b), there is a relatively large stable region away from the origin. In fact, the system can still be stable for $\tilde{\tau} = 1$ if $\tilde{v}$ is between 27 and 30.8. In fact, if $\tilde{v} = 30.5$, then $\tilde{\tau}$ can be as large as 1.5.

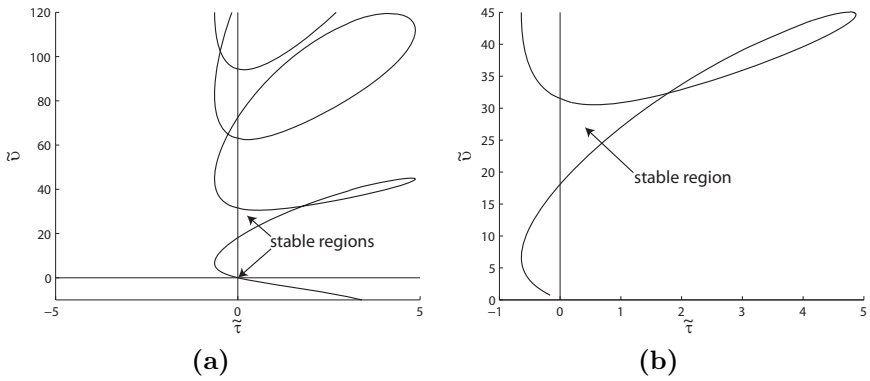

FIGURE 9. Crossing curves with respect to $\tilde{\tau}$ and $\tilde{v}$ when $\rho = 0.001$ and $\sigma = 0.0007$. (a) The zoomed-out plot shows the overall structure of the crossing curves. (b) There is a relatively large region of stability that is isolated from the origin.

Solutions of the linearized system (8) for delay values $(\rho, \sigma, \tilde{\tau}, \tilde{v})$ equal to $(0.001, 0.0007, 1, 28)$ are shown in Figure 10. As shown by our analysis, the linearized system is stable for these delay values, but converges very slowly due to the placement of the eigenvalues. The dying cancer population, C_D, remains low and constant, which is the behavior induced by the 0 eigenvalue. Despite the theoretical stability of these systems, the extremely slow rate of convergence may lead to numerical difficulties when trying to numerically evaluate the time evolution of the solutions, causing the solutions to appear periodic. This difficulty demonstrates that the resolution of using crossing curves for stability analysis exceeds that of directly evaluating the DDE system numerically.

Since this second stable region is isolated from the origin, it cannot be found using the method outlined in [2]. The method of [2] and other similar approaches work by setting one or both delays to zero and smoothly perturbing one or both delays to determine the extent of the stable region around the origin. Such methods cannot locate stable pockets that are not path connected to the origin nor can they be used to analyze the sensitivity of these isolated regions to parameter values. The isolated stable region in Figure 9(b) corresponds to large values of $\tilde{\tau}$ and $\tilde{v}$. Furthermore, by calculating the crossing curves for various values of ρ and σ, we find that unlike the stable region around the origin, the shape and location of this isolated stable region hardly changes when ρ and σ vary within the order of 10^{-2} and 10^{-3}, respectively.

Hence, as expected, in stability regions where $\tilde{\tau}$ and $\tilde{v}$ take large values, the small delays become insignificant and can be set to zero. In the same manner, the small delays are important for the stable region around the origin, because this region corresponds to very small values of $\tilde{\tau}$ and $\tilde{v}$ that are comparable to the magnitudes of the small delays, ρ and σ. These results are as expected, but

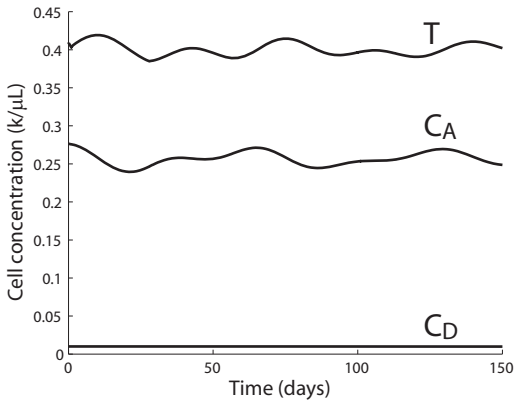

FIGURE 10. Time evolution of the linearized DDE system for $(\rho, \sigma, \tilde{\tau}, \tilde{\upsilon}) = (0.001, 0.0007, 1, 28)$. The plot shows the re-centered cell concentrations $C_A(t) + C_{A,0}$, $C_D(t) + C_{D,0}$, $T(t) + T_0$, where $C_A(t)$, $C_D(t)$, and $T(t)$ are as in (8) and T_0, $C_{A,0}$, $C_{D,0}$ correspond to fixed point 3. The system is stable, but converges very slowly.

they cannot be assumed *a priori*, and the method of stability analysis presented in this paper provides a means for verifying this claim by an explicit computation of the corresponding boundary of the stability region around the origin in the delay parameter space.

For our particular application, the delays for T cell division, $\tilde{\tau}$, and recovery from a cytotoxic process, $\tilde{\upsilon}$, are about 2 and 1 days, respectively. Hence, the isolated stable region corresponding to larger values of $\tilde{\tau}$, and $\tilde{\upsilon}$ is more relevant than the small stable region around the origin.

In the isolated stable region, the delay $\tilde{\tau}$, corresponding to $N = 2$ cell divisions, is about 1 day, which is a little fast, but still reasonable. On the other hand, the delay $\tilde{\upsilon}$, corresponding to the turn around time for T cell recovery after cytotoxic responses, is around 20 to 30 days, which is far longer than the expected 1 day turn around time.

From the perspective of medical intervention, the larger stable region away from the origin is also more interesting, because it is most likely easier to slow rates down than to speed them up. For contrast, consider the small stable region around the origin in Figure 8(b). In this region, the delays $\tilde{\tau}$ and $\tilde{\upsilon}$ are constrained to values less than 0.005 (7 min) and 0.02 (30 min), respectively, and it is almost impossible to accelerate T cell division or the T cell recovery time to these rates.

4.6. **Extension to crossing surfaces with respect to** $(\sigma, \tilde{\tau}, \tilde{\upsilon})$**.** The method developed in Section 3 uses a geometric argument to determine crossing curves with respect to two delays, and this method suggests a natural extension to the characterization of crossing surfaces of three or more delays. In particular, Figure 11(a) shows an example of the triangle geometry referred to in equations (17) and (18). In (17) and (18), the delays $\tilde{\tau}$ and $\tilde{\upsilon}$ are chosen such that the three vectors 1, $a_{\tilde{\tau}}(\rho, s)$, and $a_{\tilde{\upsilon}}(\rho, s)$ form a triangle. If we rewrite the characteristic equation (9) as

$$1 + a_1(\rho, s)e^{-\sigma s} + a_2(\rho, s)e^{-\tilde{\tau} s} + a_3(\rho, s)e^{-\tilde{\upsilon} s} = 0, \tag{36}$$

where $a_i(\rho, s) = p_i(\rho, s)/p_0(\rho, s)$, then by extension when considering the three delays σ, $\tilde{\tau}$, and $\tilde{\upsilon}$, we need the four corresponding vectors 1, $a_1(\rho, s)$, $a_2(\rho, s)$, and $a_3(\rho, s)$ to form a quadrilateral. See Figure 11(b) for a geometrical diagram.

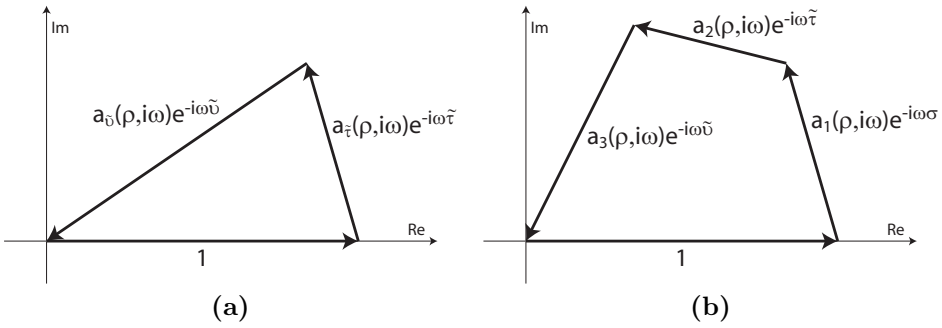

FIGURE 11. (a) Vector geometry in two dimensions. The three vectors 1, $a_{\tilde{\tau}}(\rho, s)$, and $a_{\tilde{\upsilon}}(\rho, s)$ form a triangle. (b) Vector geometry in three dimensions. The four vectors 1, $a_1(\rho, s)$, $a_2(\rho, s)$, and $a_3(\rho, s)$ form a quadrilateral.

From the four-vector geometry, we can deduce relations among the three delays σ, $\tilde{\tau}$, and $\tilde{\upsilon}$ to characterize the crossing surfaces in 3-space. Indeed, a necessary condition for the existence of solutions to (36) is that inequality (15) is not satisfied. As discussed in Section 4.5, there are two stable regions: one region around the origin and one region isolated from the origin.

Figure 12 shows the crossing surface that forms the boundary for the small stable region around the origin. As we can see, from the figure, the surface is nearly planar, so the stable region around the origin resembles a tetrahedron.

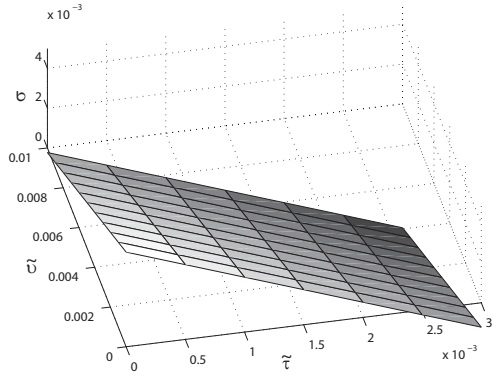

FIGURE 12. Crossing surface in $(\sigma, \tilde{\tau}, \tilde{\upsilon})$ that bounds the stable region around the origin.

It is much more difficult to plot the crossing surface that forms the boundary for the large stable region away from the origin, since this region corresponds to the loop shown in Figure 9(b), and therefore has a sharp cusp. For accurate 3-D visualization, we most likely need to consider this boundary of as the intersection

of two surfaces, rather than one continuous surface. However, we leave the details to this 3-D rendering to a future work.

Although the plot in this section provides one example of how vector geometry can be used to determine crossing surfaces in three-dimensional delay space, this approach could be extended to characterize crossing surfaces of characteristic equations of the form (36). We leave this generalization to a future work.

4.7. **Discussion.** Surprisingly, the results indicate that the stability of the controlled state, fixed point III, benefits from high values of $\tilde{v}$. This corresponds to T cells that have long turn around times after killing cancer cells. These results imply that highly reactive T cells with low turn around times may, in fact, be disadvantageous to the stability of the system. This phenomenon occurs because highly reactive T cells initially kill off cancer cells too rapidly, causing the T cell population to also decline rapidly due to lack of stimulus. The T cell population is then too low to prevent another cancer relapse resulting from the expansion of remaining cancer cells. More inert T cells, on the other hand, lead to more gradual declines of the cancer populations, which reduce the likelihood of a drastic rebound.

Hence, in this formulation of the CML model, more gradual reduction of the cancer population is favored over rapid elimination. However, we note that we did not have to deal with this issue in our previous CML work, [15], since there we studied the ruin problem, i.e., once the cancer population passes below a threshold, we consider the cancer to have been eliminated.

5. **Concluding remarks.** This paper addressed the problem of characterization of stability boundaries in some delay-parameter set for a dynamical system including *four* (independent) *delays*, system that describes the post-transplantation dynamics of the immune response to chronic myelogenous leukemia. Such a model includes two small delays, and two large delays.

In order to conduct a satisfactory stability analysis of all four delays, we implemented a geometric method to determine the crossing boundaries between stability regions in delay space. We used the method developed in [19] for two delays and extended it to four delays for our application.

The stability analysis proposed in this paper allowed us to define two types of T/C cell interactions: weak, and strong, and a quantitative measure for the weak T/C interaction was introduced, and explicitly computed. Furthermore, we have proved that the large delay values have a low influence on the stability properties in the weak cell interaction case. Next, the strong cell interaction case was analyzed in terms of stability crossing curves, and a classification of the such crossing curves is given. Finally, an example was considered for illustrating the derived results.

Acknowledgments. The authors wish to thank Odo Diekmann for useful discussions on the modeling. We would also like to thank the anonymous referees for carefully reading the manuscript and for their constructive comments.

REFERENCES

[1] M. Adimy, F. Crauste and S. Ruan, *A mathematical study of the hematopoiesis process with applications to chronic myelogenous leukemia*, SIAM J. Appl. Math., **65** (2005), 1328–1352.

[2] M. Adimy, F. Crauste and S. Ruan, *Periodic oscillations in leukopoiesis models with two delays*, J. Theor. Biol., **242** (2006), 288–299.

[3] S. Barnett, "Polynomials and Linear Control Systems," Marcel Dekker, Inc., New York, NY, USA, 1983.

[4] E. Beretta and Y. Kuang, *Geometric stability switch criteria in delay differential systems with delay dependent parameters*, SIAM J. Math. Anal., **33** (2002), 1144–1165.
[5] S. Bernard, J. Bélair and M. C. Mackey, *Oscillations in cyclical neutropenia: new evidence based on mathematical modeling*, J. Theor. Biol., **223** (2003), 283–298.
[6] S. Bernard, J. Bélair and M. C. Mackey, *Bifurcations in a white-blood cell production model*, C. R. Biol., **227** (2004), 201–210.
[7] F. G Boese, *Stability with respect to the delay: On the paper of K.L. Cooke and p. van den Driessche*, J. Math. Anal. Appl., **228** (1998), 293–321.
[8] J. W. Bruce and P. J. Giblin, "Curves and Singularities," Cambridge University Press, Cambridge, UK, 1984.
[9] S. A. Campbell, *Stability and bifurcation in the harmonic oscillator with multiple, delayed feedback loops*, Dynamics of Continuous, Discrete, and Impulsive Systems, **5** (1999), 225–235.
[10] C. I.-U. Chen, H. T. Maecker and P. P. Lee, *Development and dynamics of robust T cell responses to CML under imatinib treatment*, Blood, **111** (2008), 5342–5349.
[11] D. L. Chao, S. Forrest, M. P. Davenport and A. S. Perelson, *Stochastic stage-structured modeling of the adaptive immune system*, Proc. IEEE Comput. Soc. Bioinform. Conf., **2** (2003), 124–131.
[12] C. Colijn and M. C. Mackey, *A mathematical model of hematopoiesis–I. Periodic chronic myelogenous leukemia*, J. Theor. Biol., **237** (2005), 117–132.
[13] K. L. Cooke and P. van den Driessche, *On zeros of some transcendental equations*, Funkcialaj Ekvacioj, **29** (1986), 77–90.
[14] R. Datko, *A procedure for determination of the exponential stability of certain differential-difference equations*, Quart. Appl. Math., **36** (1978), 279–292.
[15] R. DeConde, P. S. Kim, D. Levy and P. P. Lee, *Post-transplantation dynamics of the immune response to chronic myelogenous leukemia*, J. Theor. Biol., **236** (2005), 39–59.
[16] O. Diekmann, S. A. van Gils, S. M. Verduyn-Lunel and H.-O. Walther, "Delay equations, Functional-, Complex and Nonlinear Analysis," volume **110** of Appl. Math. Sciences, Springer-Verlag, New York, NY, 1995.
[17] K. Engelborghs, T. Luzyanina and G. Samaey, *DDE-BIFTOOL v. 2.00: A Matlab package for bifurcation analysis of delay differential equations*, <http://twr.cs.kuleuven.be/research/software/delay/ddebiftool.shtml>, 2001.
[18] K. Gu, V. L. Kharitonov and J. Chen, "Stability and Robust Stability of Time-Delay Systems," Birkhäuser, Boston, MA, 2003.
[19] K. Gu, S.-I. Niculescu and J. Chen, *On stability of crossing curves for general systems with two delays*, J. Math. Anal. Appl., **311** (2005), 231–253.
[20] J. K. Hale and W. Huang, *Global geometry of the stable regions for two delay differential equations*, J. Math. Anal. Appl., **178** (1993), 344–362.
[21] J. K. Hale, E. F. Infante and F. S.-P. Tsen, *Stability in linear delay equations*, J. Math. Anal. Appl., **105** (1985), 533–555.
[22] J. K. Hale and S. M. Verduyn Lunel, "Introduction to Functional Differential Equations," volume 99 of Appl. Math. Sciences. Springer-Verlag, New York, NY, 1993.
[23] P. S. Kim, R. DeConde, D. Levy and P. P. Lee, *Post-transplantation dynamics of the immune response to chronic myelogenous leukemia*, presented at Int. Conf. on Diff. Eqs. and Applications in Math. Biology, 2004.
[24] P. S. Kim, P. P. Lee and D. Levy, *Mini-transplants for chronic myelogenous leukemia: A modeling perspective*, in "Biology and Control Theory: Current Challenges," (eds. Queinnec *et al.*), Lecture Notes in Control and Information Sciences, LNCIS 357, Springer, Berlin, 3–20, 2007.
[25] Y. Kuang, "Delay Differential Equations with Applications in Population Dynamics," Academic Press, Boston, MA, 1993.
[26] M. S. Lee and C. S. Hsu, *On the τ-decomposition method of stability analysis for retarded dynamical systems*, SIAM J. Control, **7** (1969), 242–259.
[27] N. MacDonald, "Biological Delay Systems: Linear Stability Theory," Cambridge University Press, Cambridge, UK, 1989.
[28] K. Murali-Krishna, J. D. Altman, M. Suresh, D. J. D. Sourdive, D. J. D. Zajac, J. D. Miller, J. Slansky and R. Ahmed, *Counting antigen-specific CD8+ T cells: A re-evaluation of bystander activation during viral infection*, Immunity, **8** (1998), 177–187.
[29] J. D. Murray, "Mathematical Biology: I. An Introduction," Springer-Verlag, New York, NY, 3rd edition, 2002.

[30] J. D. Murray, "Mathematical Biology: II. Spatial Models and Biomedical Applications," Springer-Verlag, New York, NY, 3rd edition, 2003.
[31] S.-I. Niculescu, "Delay Effects on Stability. A Robust Control Approach," volume 269 of *Lecture Notes in Control and Information Sciences*, Springer-Verlag, Heidelberg, Germany, 2001.
[32] N. Olgac, A. F. Ergenc and R. Sipahi, *Delay scheduling: a new concept for stabilization in multiple delay systems*, J. Vib. Control, **11** (2005), 1159–1172.
[33] G. Stépán, "Retarded Dynamical Systems: Stability and Characteristic Functions," volume **210** of "Pitman Research Notes in Mathematics," Longman Scientific & Technical, Harlow, New York, 1989.
[34] O. Toker and H. Özbay, *Complexity issues in robust stability of linear delay-differential systems*, Math. Contr. Signals Syst., **9** (1996), 386–400.

Received October 2008; revised May 2009.

E-mail address: Silviu.Niculescu@lss.supelec.fr
E-mail address: pkim@math.stanford.edu
E-mail address: kgu@siue.edu
E-mail address: ppl@stanford.edu
E-mail address: dlevy@math.umd.edu